Published in final edited form as:
Smart Mater Struct. 2011 August 1; 20(8): . doi:10.1088/0964-1726/20/8/085010.

The effect of moisture absorption on the physical properties of polyurethane shape memory polymer foams

Ya-Jen Yu[1], **Keith Hearon**[1], **Thomas S. Wilson**[2], and **Duncan J. Maitland**[1,2]

[1]Department of Biomedical Engineering, Texas A&M University, College Station, TX, USA

[2]Lawrence Livermore National Laboratory, Livermore, CA, USA

Abstract

The effect of moisture absorption on the glass transition temperature (T_g) and stress/strain behavior of network polyurethane shape memory polymer (SMP) foams has been investigated. With our ultimate goal of engineering polyurethane SMP foams for use in blood contacting environments, we have investigated the effects of moisture exposure on the physical properties of polyurethane foams. To our best knowledge, this study is the first to investigate the effects of moisture absorption at varying humidity levels (non-immersion and immersion) on the physical properties of polyurethane SMP foams. The SMP foams were exposed to differing humidity levels for varying lengths of time, and they exhibited a maximum water uptake of 8.0% (by mass) after exposure to 100% relative humidity for 96 h. Differential scanning calorimetry results demonstrated that water absorption significantly decreased the T_g of the foam, with a maximum water uptake shifting the T_g from 67 °C to 5 °C. Samples that were immersed in water for 96 h and immediately subjected to tensile testing exhibited 100% increases in failure strains and 500% decreases in failure stresses; however, in all cases of time and humidity exposure, the plasticization effect was reversible upon placing moisture-saturated samples in 40% humidity environments for 24 h.

1. Introduction

Shape memory polymers (SMPs) are smart materials that can store a metastable geometry or geometries and then actuate to a primary geometry after introduction to a stimulus such as heat or moisture. Because of this capability, SMPs have attracted increasing attention from the scientific community and are being proposed for numerous applications in diverse arenas, ranging from the aerospace to biomedical industries [1]. SMP foams are of particular interest because they exhibit large volume expansions upon actuation [2]. Raytheon is currently investigating SMP foams for implementation in aerospace applications, and an SMP foam-based biomedical implant device for treating aneurisms is currently being developed [3]. Neat SMPs and SMP foams can be manufactured to respond to specific stimuli such as heat [4], light [5], electric fields [6], magnetic fields [7], and moisture [8]. Currently, thermo-responsive SMPs have received the most attention for implementation in device-based applications [9].

Traditional thermo-responsive, two-shape SMPs are heated above a transition temperature, T_{trans}, deformed, and subsequently cooled below T_{trans} to fix a secondary geometry. The secondary geometry is maintained because thermodynamic barriers prevent the polymer chains from relaxing and returning to their original state of higher entropy, which the chains automatically assumed during initial polymerization or processing. T_{trans} can be a glass

djmaitland@tamu.edu.

transition temperature (T_g), a crystalline melt temperature (T_m), or another transition temperature [4]. After heating above T_{trans}, a deformed SMP returns to its high-entropy state, which is the original geometry. At the molecular level, netpoints such as covalent crosslinks, crystalline phases, and chain entanglements enhance the integrity of the SMP system by keeping polymer chains from sliding past one another while the polymer is heated above T_{trans} [10].

Previous studies on polyurethane SMPs have focused on synthesis [11–12], structural modeling [13], thermo-mechanical characterization [14], and moisture effects [15]. In particular, Yang investigated the effects of moisture absorption on the glass transition temperature and corresponding stress-strain behavior of neat polyurethane SMPs. Yang's studies revealed that absorbed water in polyurethanes falls into two categories: bound water and free water. Bound water, which acts as a plasticizer by occupying hydrogen bonding sites between interchain carbamate N-H and C=O groups, significantly lowers T_g and consequently significantly alters stress-strain behavior. Free water, on the other hand, has much less of a plasticizing effect for polyurethanes.

Although Yang's studies and those of others have effectively characterized the effects of moisture absorption on the thermal and thermo-mechanical properties of urethane SMPs [16–17], these studies have been limited to neat polyurethane SMPs. Research related to the effect of moisture exposure on polyurethane foams has examined moisture diffusion rate and mechanical property changes [18–19]; however, the effect of moisture uptake on the shape memory behavior of polyurethane foams has yet to be evaluated.

In this study, we evaluated the effect of moisture absorption on the T_g and stress/strain behavior of polyurethane SMP foams made from a urethane SMP composition described in Wilson 2007 [11]. Moisture uptake at different temperatures and humidity levels was measured using thermogravimetric analysis (TGA) and mass ratio analysis. Fourier transform infrared (FTIR) spectroscopy was used to analyze the interactions of the absorbed water with the urethane foams. Moisture-induced T_g effects were measured using differential scanning calorimetry (DSC), and the effect of water uptake on the stress/strain and shape memory behavior of the foams was evaluated by strain to failure and free strain recovery experiments.

2. Experimental

2.1. Polyurethane foam synthesis and sample preparation

Polyurethane SMP foams were prepared based on a technique developed by Dr. Thomas S. Wilson at Lawrence Livermore National Laboratory. Prepolymers were made from hexamethylene diisocyanate (HDI, 98%, TCI America), N,N,N',N'-tetrakis(2-hydroxypropyl) ethylenediamine (HPED, 98%, TCI America), and triethanolamine (TEA, 99%, Sigma-Aldrich). Foams were formulated from the prepolymers by adding the following surfactants, catalysts, and blowing agents in a Flackteck 150 DAC speed mixer for 15 s at 3400 rpm: DC-5179 (Air Products), DC-I990 (Air Products), T131 (Air Products), BL-22 (Air Products), DI water and Enovate (Honeywell Corp.) For foaming, an overall NCO/OH ratio of 1.05 was used.

After sample preparation, the polyurethane foams were dried at 90 °C for 12 h at 1 torr to remove residual moisture. The samples were then placed in a CSZ MCBH-1.2-.33-.33-H/AC environmental chamber at a controlled temperature of 25 °C, with controlled humidities of 40 %, 60 %, and 80% for time periods of 0.5 h, 1 h, 2 h, 3 h, 4 h, 5 h, 6 h, 12 h, 24 h, 48h, and 96 h. For sample preparation at 100% humidity, the samples were immersed into a water bath at control temperatures of 25 °C or 37 °C for time periods of 12 h, 24 h, 48 h, and 96 h.

2.2. Characterization

2.2.1. Moisture uptake—TGA analysis was used to measure the water uptake of samples exposed to various humidities for time periods of 12 h, 24 h, 48 h, and 96 h. TGA was run on 10–15 mg samples in a TA Instruments Q80 thermogravimetric analyzer. TGA samples, tested in triplicate, were heated from 30 °C to 400 °C at 10 °C/min. In order to accurately evaluate the time it took the foams to reach moisture saturation at each humidity level, a second set of foam samples was subjected to mass ratio analysis. Five specimens of each sample were massed, exposed to the different humidity levels for 0.5 h, 1 h, 2 h, 3 h, 4 h, 5 h, and 6 h, and re-massed immediately after removal from the environmental chamber.

2.2.2. Glass transition temperature shift—DSC experiments were run using a TA Instruments Q200 differential scanning calorimeter from −40 °C to 80 °C at 10 °C/min on 5–10 mg samples to evaluate the effect of moisture absorption on T_g. To determine whether the T_g shift was reversible, samples that had been exposed to various humidity levels for 96 h were put back in the environmental chamber at 40% humidity for 1 day, 2 days, and 5 days, after which DSC experiments were run with the same experimental procedures described above.

2.2.3. Infrared band shift—The interactions between absorbed water molecules and hydrogen-bonded N-H and C=O groups were analyzed using a Bruker Tensor 27 FTIR spectrometer. A control foam sample that had not been exposed to moisture was run in addition to the humidified samples. FTIR spectra were collected by averaging 150 scans with a resolution of 4 cm^{-1} and a wavenumber range of 600 cm^{-1} to 4000 cm^{-1}. To determine whether the shifts in the IR spectra were reversible, samples that had been exposed to various humidity levels for 96 h were put back in the environmental chamber at 40% humidity for 1 day, 2 days, and 5 days, after which FTIR experiments were run with the same experimental procedures described above.

2.2.4. Stress/strain behavior—Strain to failure experiments were carried out on 60 x 15 x 6 mm polyurethane foam samples using an MTS Insight 30 Universal Tensile Tester. In accordance with ASTM D638 Standard Test Method for the Tensile Properties of Plastics, samples were mounted in epoxy blocks and exposed to different humidity levels for 96 h. These samples were then immediately subjected to strain to failure experiments at a constant strain rate of 50 mm/min at 25 °C. To determine whether the moisture-induced changes in stress-strain behavior were reversible, samples that had been exposed to various humidity levels for 96 h were put back in the environmental chamber at 40% humidity for 1 day, after which strain to failure experiments were run with the same experimental procedures described above.

2.2.5. Shape memory effect—Free strain recovery experiments were carried out on 60 x 15 x 6 mm polyurethane foam samples in an MTS Insight 30 Universal Tensile Tester with a thermal chamber. In accordance with ASTM D3574-08 Standard Test Method for Polyurethane Foams, samples were mounted on epoxy blocks and exposed to 100% humidity for 96 h (one sample at 25 °C, and another at 37 °C). The samples were then gripped in the tensile tester, heated to 80 °C at 1 °C/min, and strained to 15%, 25%, and 35%. The strained samples were then cooled to 25 °C at 1 °C/min to fix the respective strains. Then, for free strain recovery, the bottoms of the samples were unclamped inside the thermal chamber, and the samples were heated to 80 °C at 1 °C/min to determine recoverable strain, which was measured by a laser extensometer. Percent recoverable strain, or recovery ratio, is calculated according to Equation (1),

$$\text{Recovery Ratio} = \text{Recovered length} / \text{Initial length} \times 100 \quad (1)$$

3. Results and discussion

3.1. Moisture uptake

Results for percent moisture uptake as measured by TGA and mass ratio analysis are provided in figures 1 and 2, respectively. For 40%, 60%, and 80% relative humidities, moisture absorption increased with humidity exposure time until 6 h, after which it generally remained constant. For the samples exposed to 100% humidity (i.e., immersion in water), reaching maximum water uptake took longer. As figure 1 demonstrates, the maximum water uptake after 96 h at 25 °C in the 100% relative humidity environment was 8%, and this value did not change significantly when the temperature in the environmental chamber was increased to 37 °C. However, increased temperature did increase the moisture absorption rate [20], as figure 1 shows. The 37 °C sample reached maximum water uptake at 20 h, while the 25 °C sample did not reach maximum water uptake until 96 h. As expected, moisture absorption and moisture saturation levels were dependent on moisture exposure time, humidity level, and temperature. Our results prove that moisture saturation is dependent on the ambient humidity level that the greater the humidity level result in the greater the possible water uptake [21].

Figures 1 and 2 show the moisture absorption with water immersion is different from non-immersion water absorption. Even though the environmental chamber provides 100% humidity, the 100% humidity absorption is not equivalent to water immersion. Our finding agrees with Loos et al., who showed that different environmental exposure affects the water absorption behavior [22].

3.2. Glass transition temperature shift

The glass transition temperatures of all samples decreased upon moisture absorption, as shown in figure 3. After 12 h, the T_g's of the foams generally reached a plateau. A maximum shift in T_g occurred for the 100% humidity foams (both 25 °C and 37 °C), where the T_g dropped from 67 °C to 5 °C after 96 h. The moisture effects on T_g were reversible, as shown in figure 4. Samples that were exposed to humidity for 96 h and then placed in the environmental chamber at 40% humidity exhibited significant moisture loss after 1 day. The absorbed moisture for all samples was approximately the same after one day (2.2%). This value of 2.2% corresponds to the initial absorbed moisture value for the foam exposed to 40% relative humidity that is plotted in figure 1. This moisture loss was accompanied by an increase in T_g: after being placed in the environmental chamber at 40% humidity for one day, the T_g's of all samples increased to roughly the same value: 42 °C, the T_g value for the initial foam exposed to 40% humidity that is plotted in figure 3.

3.3. Infrared band shift

The control foam sample that was not exposed to humidity exhibited a bond N-H stretch intensity peak at 3307 cm^{-1}. As figure 5 indicates, the bond N-H stretch intensity peaks were shifted both to higher wavenumbers and higher intensities with increasing moisture absorption, with the 100% humidity samples exhibiting N-H stretch intensity peaks at approximately 3332 cm^{-1}. Figure 6 shows the effect of absorbed moisture on the carbamate and urea C=O stretch intensity peaks, which occur at 1687 cm^{-1} and 1647 cm^{-1}, respectively. Although increased water content resulted in increased intensities for the respective C=O peaks, observable shifts in wavenumber did not occur.

In a moisture-free polyurethane foam, hydrogen bonding occurs between carbamate N-H and C=O groups. After moisture absorption, the hydrogens in water molecules can either form hydrogen bonding bridges between two carbamate C=O groups or occupy the hydrogen bonding sites at carbamate N-H groups [23]. Hydrogen bonds formed with the N-H groups cause the N-H infrared bands to increase in intensity and shift to higher wavenumbers. Such behavior is apparent in the IR spectra in figure 5 for our polyurethane SMP foams. In contrast, the hydrogen bonds formed with the C=O groups cause the C=O infrared bands to increase in intensity and shift to lower wavenumbers [24]. Although our foams exhibited increased carbamate C=O peak intensities with increasing moisture absorption, no discernable shift in wavenumber was apparent.

One possible explanation for this behavior is that the chemical structure of the polyurethane foams characterized in this work is significantly different from that of other urethanes: there are no traditional hard and soft segments. Also, our foaming process includes the addition of water, which results in an increased urea content and even more hydrogen bonding interactions. The foams are entirely comprised of 6-carbon-long diisocyanates and low-molecular weight tri-and-tetrafunctional alcohols, so the ratio of carbamate and urea linkages to the total number of molecules in the polymer is much higher than that of an SMP with an oligomeric soft segment. Since each carbamate linkage has two hydrogen bonding sites (C=O and N-H; three in the case of urea linkages), our foams have significantly more hydrogen bonding sites than a polyurethane with, for example, a polyethylene oxide or polybutadiene soft segment. The urethane and urea in this study could have so great a number of bound carbonyls before moisture absorption that, even after maximum moisture absorption, there could still be no discernable shift in wavenumber. This theory could also explain why there are no apparent free carbonyl peaks in our IR spectrum. Since bound carbonyl peaks are significantly broader than free carbonyl peaks, it is possible that the broadness and intensity of the bond carbonyl peaks makes it impossible to observe the free carbonyl peaks [25–26].

We found the moisture-induced shifts of the N-H peaks in the IR spectra peak to be reversible. Yang, et al. demonstrated such reversibility by driving off absorbed moisture by heating polyurethane samples [8]. We demonstrated a similar effect by placing moisture-saturated samples in a lower humidity environment (40% humidity). The N-H peaks shift back to 3307 cm^{-1}, and the C=O peaks shift back to lower intensities after exposure to 40% humidity at 25 °C (the data does not show). Although moisture appears to evaporate from our foams with relative ease (Yang, et al. heated neat polyurethane at different temperatures to drive off moisture), this observation does not necessarily indicate that there are weaker hydrogen bonding interactions in our urethane than in other urethanes. Urethane foams have significantly more surface area than neat urethane films, so the significant moisture evaporation from the foams could simply be a result of increased surface area.

3.4. Stress/strain behavior

Tensile testing data for all samples is provided in Table 1. Strain to failure results demonstrated that absorbed moisture significantly plasticized the urethane foams [27], although this plasticization effect proved to be reversible. The samples that were exposed to various humidities and then placed in the room temperature for 1 day exhibited failure strains on the order of 20% and failure stresses on the order of 50 kPa. The samples were exposed to 100% humidity, and then immediately tested within 1 h exhibited failure strains on the order of 30–40% and failure stresses on the order of 15 kPa. Similar trends occurred for Young's modulus values. The representative stress-strain curve for PU foams is shown in figure 7; representing water molecules acting as plasticizer. This plasticization increased the breaking strain and decreased the failure stress and Young's modulus. The observed

plasticization effect was in accordance with the results of Yang's studies on the effects of moisture on the stress/strain behavior of neat polyurethanes.

3.5. Shape memory effect

Free strain recovery results for samples exposed to 100% humidity at 37 °C for 96 h are provided in figure 8. For 15% and 25% strains, the observed recovery ratio was approximately 95%. For 35% strains, the recovery ratio decreased to 87%. Since the polyurethane foams characterized in this work were highly crosslinked, even strains as low as 35% could result in localized permanent deformations and destruction of foam cells [28].

4. Conclusions

The water uptake of the polyurethane SMP foams characterized in this work increased with increased humidity exposure time, increased humidity, and increased temperature. The maximum water uptake was 8%, which occurred after exposure to 100% humidity for 96 h at room temperature and for 20 h at 37 °C. At humidities less than or equal to 80%, moisture saturation occurred after 6 h.

The T_g of the polyurethane foams decreased upon moisture absorption, and a maximum shift from 67 °C to 5 °C occurred after 8% water uptake. This T_g shift affected a transformation from glassy to viscoelastic behavior when the SMP foams were subjected to tensile testing at 25 °C. Both the T_g shifts and the resulting mechanical behavior transformations were reversible upon placing the foams in a 40% humidity environment for 24 h.

The tensile stress-strain curve shows the water molecules are penetrating the inner structure of PU foams, acting as plasticizer. The water molecules generate hydrogen bonding between N-H and C=O groups, interrupting the original hydrogen bonds to permit polymer chains to move freely and thereby increase in the breaking strain and decrease in the failure stress and Young's modulus.

Recovery ratios approaching 100% for samples strained to 25% or less demonstrate that the SMP foams characterized in this work are potentially useful for applications where complete tensile strain recovery is necessary.

Acknowledgments

We thank Amanda Connor and Brent Volk for discussion and technical support. This work was supported by the National Institutes of Health/National Institute of Biomedical Imaging and Bioengineering Grant R01EB000462 and partially performed under the auspices of the U.S. Department of Energy by Lawrence Livermore National Laboratory under Contract DE-AC52-07NA27344.

References

1. Behl M, Lendlein A. Shape-memory polymers. Mater Today. 2007; 10:20–28.
2. Huang WM, Lee CW, Teo HP. Thermomechanical behavior of a polyurethane shape memory polymer foam. J Intell Mater Syst Struct. 2006; 17:753–60.
3. Maitland DJ, Small W, Ortega JM, Buckley PR, Rodriguez J, Hartman J, Wilson TS. Prototype laser-activated shape memory polymer foam device for embolic treatment of aneurysms. J Biomed Opt. 2007; 12:030504. [PubMed: 17614707]
4. Lendlein A, Kelch S. Shape-memory polymers. Angew Chem Int Ed. 2002; 41:2034–57.
5. Lendlein A, Jiang H, Junger O, Langer R. Light-induced shape-memory polymers. Nature. 2005; 434:879–82. [PubMed: 15829960]
6. Sahoo NG, Jung YC, Goo NS, Cho JW. Conducting shape memory polyurethane-polypyrrole composites for an electroactive actuator. Macromol Mater Eng. 2005; 290:1049–55.

7. Buckley PR, Mckinley GH, Wilson TS, Small W, Benett WJ, Bearinger JP, Mcelfresh MW, Maitland DJ. Inductively heated shape memory polymer for the magnetic actuation of medical devices. IEEE Trans Biomed Eng. 2006; 53:2075–83. [PubMed: 17019872]
8. Yang B, Huang WM, Li C, Li L. Effects of moisture on the thermomechanical properties of a polyurethane shape memory polymer. Polymer. 2006; 47:1348–56.
9. Small W, Singhal P, Wilson TS, Maitland DJ. Biomedical applications of thermally activated shape memory polymers. J Mater Chem. 2010; 20:3356–66. [PubMed: 21258605]
10. Behl M, Razzaq MY, Lendlein A. Multifunctional shape-memory polymers. Adv Mater. 2010; 22:3388–410. [PubMed: 20574951]
11. Wilson TS, Bearinger JP, Herberg JL, Marion JE, Wright WJ, Evans CL, Maitland DJ. Shape memory polymers based on uniform aliphatic urethane networks. J Appl Polym Sci. 2007; 106:540–51.
12. Hearon K, Gall K, Ware T, Maitland DJ, Bearinger JP, Wilson TS. Post-Polymerization Crosslinked Polyurethane Shape-Memory Polymers. J App Poly Sci. 2010; 121:141–53.
13. Volk BL, Lagoudas DC, Chen Y-C. Analysis of the finite deformation response of shape memory polymers: II. 1D calibration and numerical implementation of a finite deformation, thermoelastic model. Smart Mater Struct. 2010; 19:075006.
14. Tobushi H, Hara H, Yamada E, Hayashi S. Thermomechanical properties in a thin film of shape memory polymer of polyurethane series. Smart Mater Struct. 1996; 5:483–91.
15. Yang B, Huang WM, Li C, Lee CM, Li L. On the effects of moisture in a polyurethane shape memory polymer. Smart Mater Struct. 2004; 13:191–5.
16. Xu B, Huang WM, Pei YT, Chen ZG, Kraft A, Reuben R, De Hosson JTM, Fu YQ. Mechanical properties of attapulgite clay reinforced polyurethane shape-memory nanocomposites. Eur Polym J. 2009; 45:1904–11.
17. Pretsch T, Jakob I, Müller W. Hydrolytic degradation and functional stability of a segmented shape memory poly(ester urethane). Polym Degrad Stab. 2009; 94:61–73.
18. Oertel, G. Polyurethane Handbook. New York: Hanser; 1985.
19. Zhao D, Little JC, Cox SS. Characterizing polyurethane foam as a sink for or source of volatile organic compounds in Indoor Air. J Environ Eng. 2004; 130:983–89.
20. Bassirirad H, Radin JW, Matsuda K. Temperature-dependent water and ion transport properties of barley and sorghum roots : I. relationship to leaf growth. Plant Physiol. 1991; 97:426–32. [PubMed: 16668404]
21. Avilés F, Aguilar-Montero M. Moisture absorption in foam-cored composite sandwich structures. Polym Compos. 2010; 31:714–22.
22. Loos, Alfred C.; Springer, George S.; Sanders, Barbara A.; Tung, RW. Moisture absorption of polyester-E glass composites. J Compos Mater. 1980; 14:142–54.
23. Lim LT, Britt IJ, Tung MA. Sorption and transport of water vapor in nylon 6,6 film. J Appl Polym Sci. 1999; 71:197–206.
24. Yen F-S, Lin L-L, Hong J-L. Hydrogen-bond interactions between urethane-urethane and urethane-ester linkages in a liquid crystalline poly(ester-urethane). Macromolecules. 1999; 32:3068–79.
25. Mattia J, Painter P. A Comparison of hydrogen bonding and order in a polyurethane and poly(urethane-urea) and their blends with poly(ethylene glycol). Macromolecules. 2007; 40:1546–54.
26. Yilgör E, Burgaz E, Yurtsever E, Yilgör I. Comparison of hydrogen bonding in polydimethylsiloxane and polyether based urethane and urea copolymers. Polymer. 2000; 41:849–57.
27. Dhakal HN, Zhang ZY, Richardson MOW. Effect of water absorption on the mechanical properties of hemp fibre reinforced unsaturated polyester composites. Compos Sci Technol. 2007; 67:1674–83.
28. Volk BL, Lagoudas DC, Chen Y-C, Whitley KS. Analysis of the finite deformation response of shape memory polymers: I. Thermomechanical characterization. Smart Mater Struct. 2010; 19:075005.

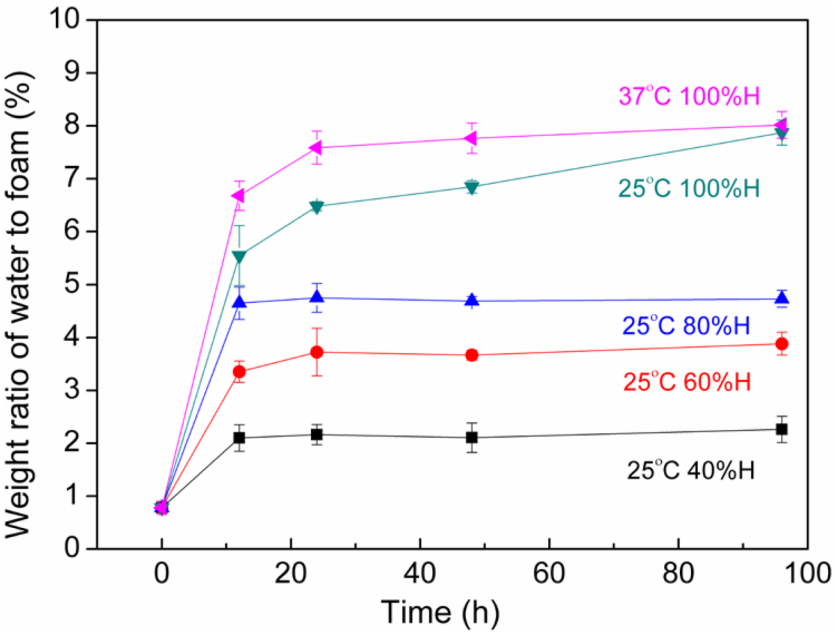

Figure 1.
The effect of humidity exposure time up moisture absorption, measured by TGA.

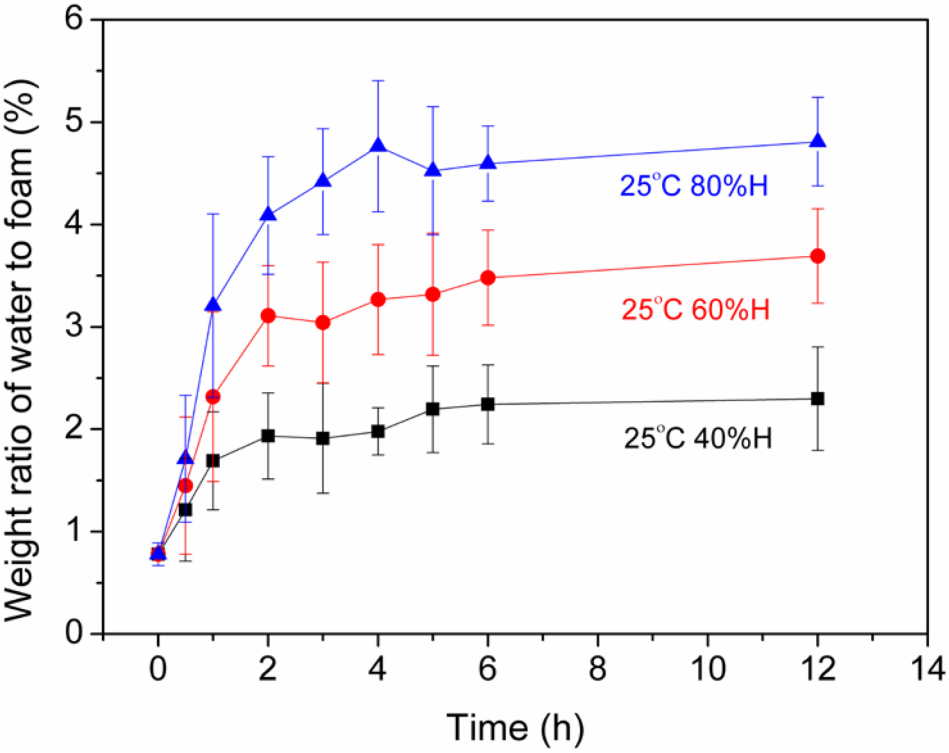

Figure 2.
The effect of humidity exposure time on moisture exposure time, measured by mass ratio analysis.

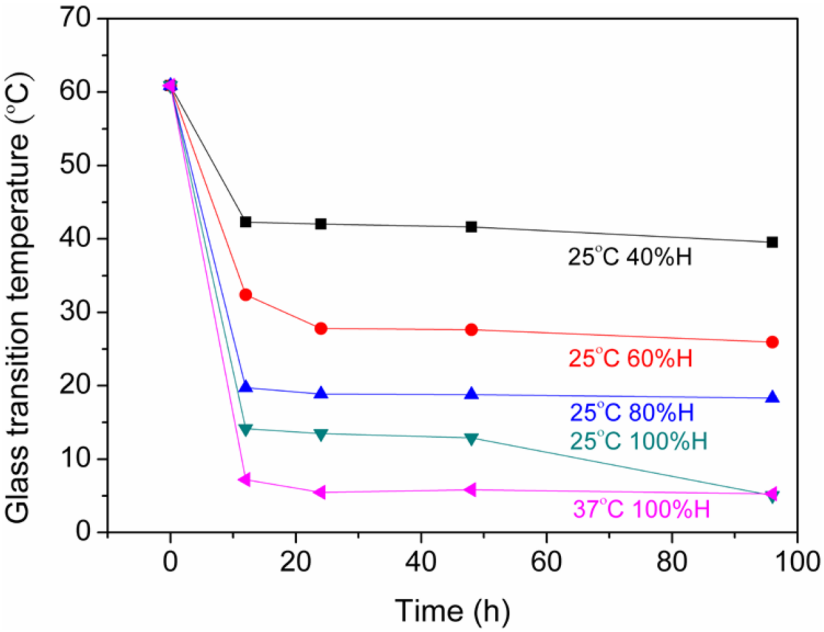

Figure 3.
The effect of moisture absorption of T_g.

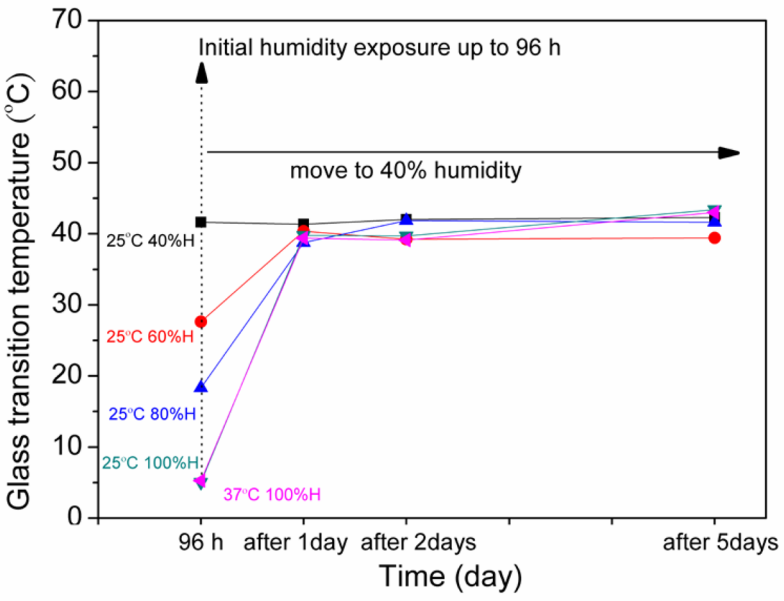

Figure 4.
The effect of controlled moisture on reversible T_g.

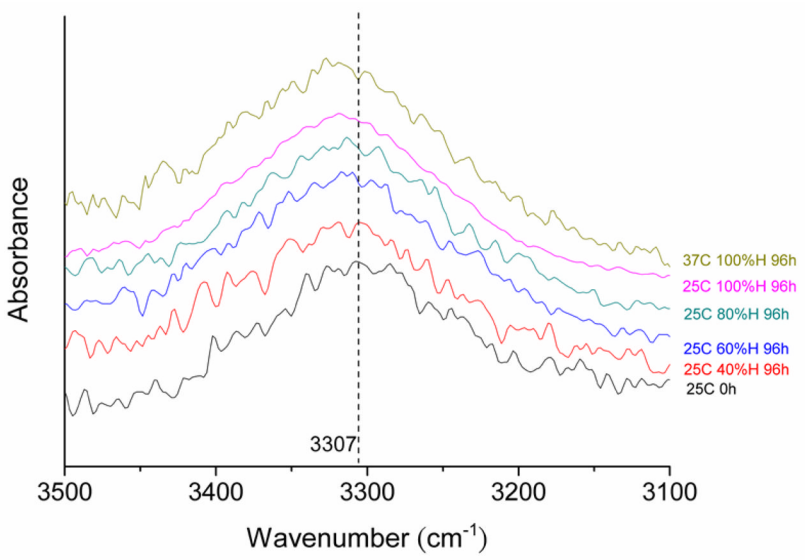

Figure 5.
FTIR spectra of N-H stretching region of polyurethane foam with differing water uptake levels.

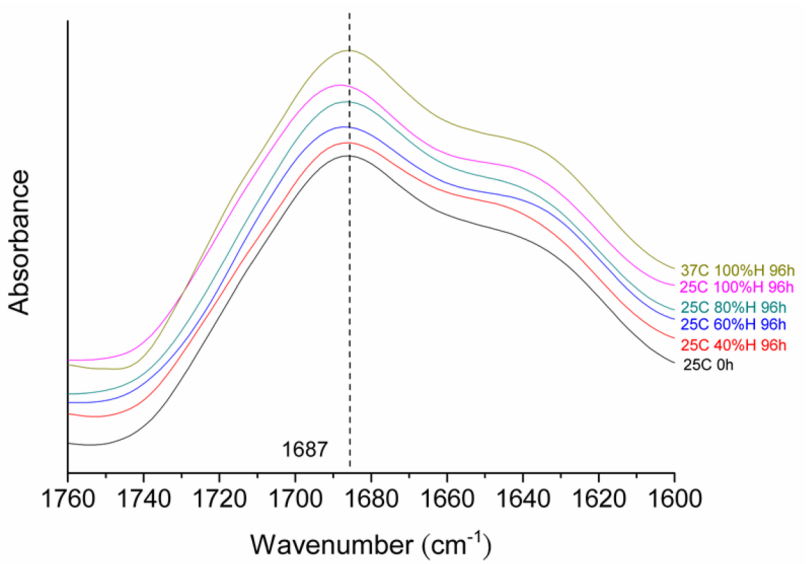

Figure 6.
FTIR spectra of C=O stretching region of polyurethane foam with differing water uptake levels.

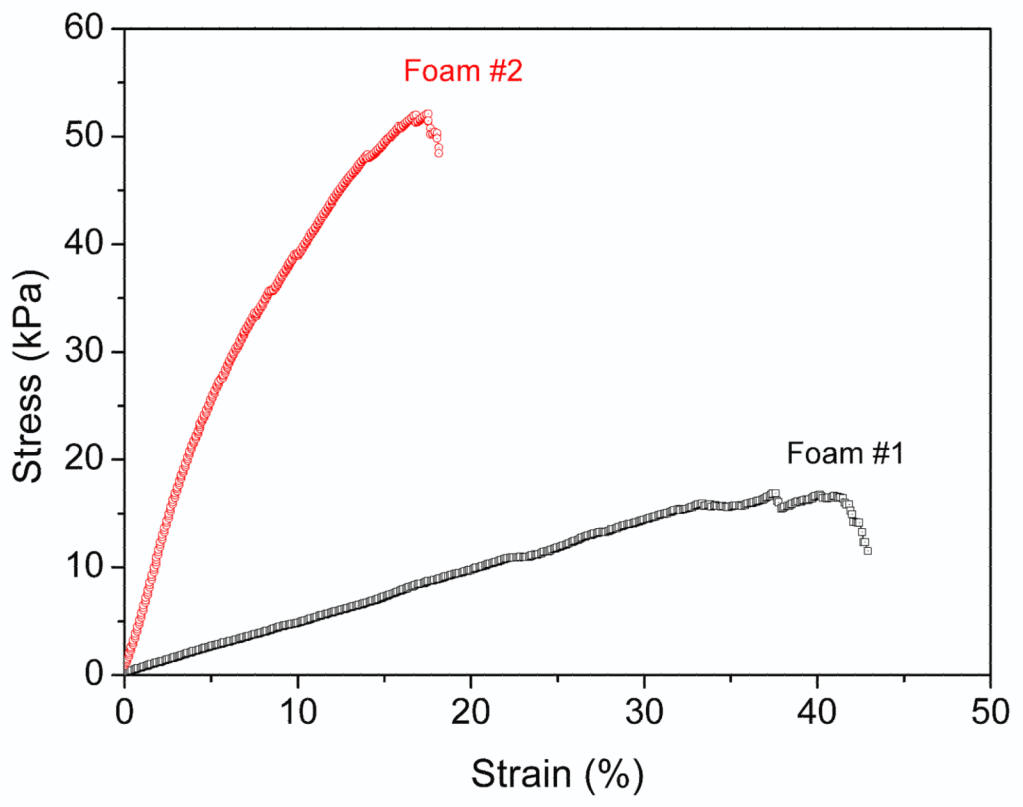

Figure 7.
Representative tensile stress-strain curve for the PU foams data in Table 1.
(Foam #1: water uptake for 96 h at 37 °C after testing; Foam #2: the same test run after 24 h in room temperature, approximately 20 °C and 40% relative humidity, throughout testing.)

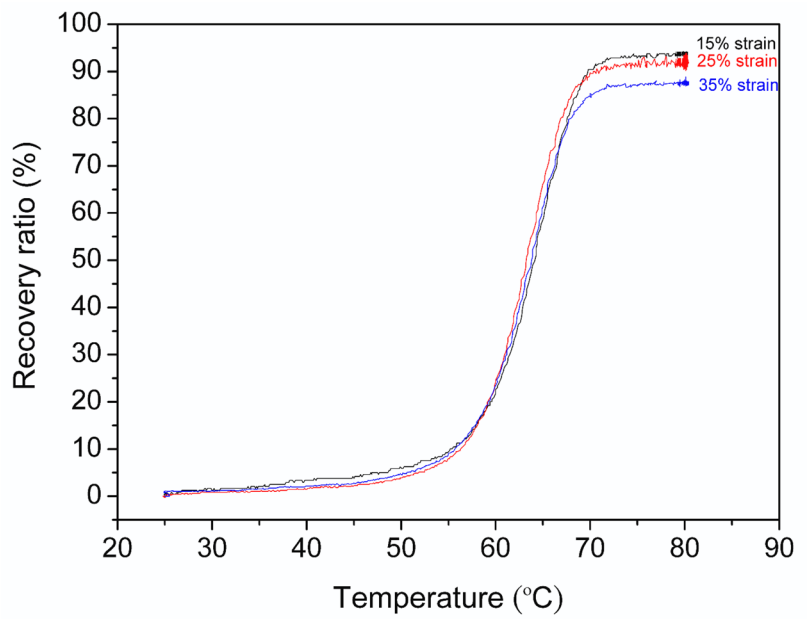

Figure 8.
Recovery upon heating.

Table 1

	Breaking strain (%)	Breaking tensile strength (kPa)	Young modulus (kPa)
25°C-40%H-96h-24h STP*	21 ± 7	52 ± 11	281 ± 117
25°C-60%H-96h-24h STP*	18 ± 5	50 ± 12	282 ± 56
25°C-80%H-96h-24h STP*	18 ± 6	43 ± 13	275 ± 143
25°C-100%H-96h-24h STP*	23 ± 5	55 ± 13	247 ± 77
37°C-100%H-96h-24h STP*	21 ± 6	43 ± 11	226 ± 108
25°C-100%H-96h	31 ± 1	17 ± 1	52 ± 2
37°C-100%H-96h	41 ± 12	14 ± 5	35 ± 13

* STP was measured at room temperature, approximately 20 °C and 40% relative humidity.